Movable Payload on Various Conditions of Two-Wheeled Double Links Wheelchair Stability Control Using Enhanced Interval Type-2 Fuzzy Logic

NURUL FADZLINA JAMIN[1], NOR MANIHA ABDUL GHANI [ID][1], AND ZUWAIRIE IBRAHIM[2]

[1]Faculty of Electrical & Electronics Engineering Technology, Universiti Malaysia Pahang, Gambang 26600, Malaysia
[2]College of Engineering, Universiti Malaysia Pahang, Gambang 26600, Malaysia

Corresponding author: Nor Maniha Abdul Ghani (normaniha@ump.edu.my)

ABSTRACT This paper presents investigations of control strategies for a two-wheeled wheelchair with a movable payload on various conditions using a double-link inverted pendulum concept. The wheelchair system is modeled in the SimWise 4D (SW4D) with its optimized control parameters determined using the Spiral Dynamic Algorithm (SDA) while being controlled by the proposed Interval Type-2 Fuzzy Logic Controller (IT2FLC). The robustness of the proposed controller in terms of maintaining the system's stability while the wheelchair is standing in an upright position is tested under multiple circumstances. These included utilizing varying directions and applying magnitudes of external disturbances to the developed system with a movable payload (upward and downward) and testing the system's forward and backward motions on a flat surface and the motions on an inclined surface. Ultimately, the two-wheeled wheelchair which adopts the proposed controller had shown a 68% and 77% reduction in the angular positions of Link1 and Link2, a 94% reduction in torques for both Link1 and Link2, and more than 98% reduction in traveling distance compared to the Fuzzy Logic Control Type-1 (FLCT1) controller which was used in the previous design. Moreover, the current work has taken into consideration the heightened nonlinearities and complexity of an additional moving payload on various conditions to represent more degree of freedom (DOF), compared to the fixed payload in the previous design with less DOF. This further rectifies that the enhanced IT2FLC had outperformed FLCT1 in handling nonlinearities and uncertainties, for the case of a two-wheeled wheelchair system with a movable payload.

INDEX TERMS Two-wheeled wheelchair, movable payload of a double-link inverted pendulum, optimized interval type-2 fuzzy logic, stability of the two-wheeled system.

I. INTRODUCTION

A wheelchair is known to be a vital tool in providing mobility for the elderly, as well as the disabled community, to travel between destinations. It is vital to ensure that wheelchair users can perform their daily routines independently, provided they remain secured and protected from any risk during the usage of the wheelchair. Therefore, apart from the practicality of its design, priority is placed upon the safety aspects of a wheelchair to ensure the safety and comfort of fellow

users with a specific emphasis on obtaining shorter traveling distances and enhanced stability with reduced torques, following both foreseen and unforeseen disruptions.

Essentially, the standard configuration for a wheelchair is designed in a normal four-wheeled form. While providing mobility, the standard four-wheeled wheelchairs were found to have some limitations due to their control mechanism and their design, mainly the lack of height control that limits its level for vertical reach, and the bulky design that presents difficulties to move in narrow spaces. Thereby, this model was further enhanced, which enables a two-wheeled transformation that improves its performance, while

The associate editor coordinating the review of this manuscript and approving it for publication was Yang Tang [ID].

overcoming these downfalls. In securing the user's upright position when switching between a four-wheeled to a two-wheeled wheelchair, this system usually requires an initial high torque to maintain stability in lifting the front wheels, and this will indirectly cause a shorter battery life, and it can be easily damaged.

Alternatively, a two-wheeled wheelchair has presented a degree of advantage over both the standard four-wheeled wheelchair and the transformational wheelchair that switches between two and four wheels. This accounts for its comparatively heightened stability in an upright position that disregards the initial high torque as required in four-wheeled wheelchairs while being sufficiently compact to maneuver across narrow spaces safely. Along with height control, it merely allows users to extend the vertical reach further. Moreover, there are added advantages if the users use a wheelchair with a movable payload system introduced in this paper, which should be noticed. The users can have direct eye-to-eye contact during conversations with normal people at standard height. This is crucial as it can increase the self-confidence level of the disabled user. The disabled users can also reach things at higher places such as shelves independently. This allows the users to refrain from burdening other people around them to perform daily routine activities on their own. However, a higher level of height comes with the expense of stability in the case of movable payload.

A two-wheeled wheelchair based on the double-link inverted pendulum system is known to be highly complex, nonlinear and unstable. Thus, it could potentially cause difficulties in controlling its stability during vertical maneuvering with a movable payload - upward and downward motions of the seat. With the development of two-wheeled wheelchairs for greater user flexibility, existing control strategies have proven to be a nuisance due to heightened fluctuations ensuing external disruptions.

Ahmad et al. proposed the use of Linear Quadratic Regular (LQR) to lift the front wheels of the four-wheeled wheelchair, transforming it into a two-wheeled wheelchair while stabilizing the system at an upright position, based on mathematical derivations. However, this approach fails to achieve satisfactory performance in terms of overshoot, highlighting the need for systematic tuning to resolve this issue [1].

The Proportional Integral Derivative (PID) approach has further been applied in [2] to control the stability of a wheelchair in the case of climbing stairs. The results have also presented a satisfactory performance in terms of system stability for both ascending and descending stairs. A significantly higher initial wheel torque has been recorded while taking on the act of ascending, with a value of 250Nm on the first ascending step, further increased to 300Nm on the following steps.

In view of handling incoming disruptions, a locking mechanism has been proposed in the wheelchair system [3], which is activated once the wheelchair is on two wheels. With a simulated disruption of 1000N in force at the back of the

wheelchair, the mechanism enables stabilization in an upright position throughout the process, with the application of the FLCT1 controller. This has proven to be essential as a safety precaution that prevents wheelchair users from falling. However, the nonlinearities of the system have decreased from a double-link to a single-link inverted pendulum system once the wheelchair is on two wheels.

As highlighted by [7], a two-wheeled wheelchair is shown to enable steering motions and maneuvers within a narrow space, through the use of Modular FLCT1. Herewith, proportional compensators have been implemented alongside the fore-mentioned modular FLCT1 to stabilize the wheelchair during the steering motion. A similar application is further extended by the author, in the performance of both forward and backward motions [4].

Additionally, FLCT1 has also been tested with several types of positive and negative disturbances under 10s repetitions, as shown in [6], [9]. The switching mechanism is hereby implemented alongside FLCT1 to control the lifting and stabilizing integration, maintaining the value within the threshold of $\pm 5°$. Various disturbances between the force of $\pm 100N$ to $\pm 300N$ have been applied to the back of the chair under 10s repeated intervals. A single force of $\pm 2000N$ has also been randomly applied once, within the intervals, to test the chair's capability in handling sudden incoming uncertainties. The results have shown successful attempts for FLCT1 in handling uncertainties, without disrupting the wheelchair's stability at an upright position. A further traveling distance of 2m has been recorded due to the uncertain disruption, with higher fluctuations recorded following the influence of a negative force, which prolongs the settling time.

Following this, Rahman et al. proposed the use of the LQR controller to control the stability of a two-wheeled mobile robot. The paper has adopted the 4D software, while focused on modeling the robot using a derivation of the state-space model. As discovered, the controller has presented successful results in controlling the stability of Link1 and Link2 at an upright position [14]. However, shortcomings were discovered in this study with the LQR approach being impractical in handling unforeseen disruptions, while the inclusion of human weight has been neglected in this experiment.

On another note, the use of a PID controller is proposed to control the stability of vehicles with an extendable rod on two-wheels [13]. In this case, the Genetic Algorithm has been applied to seek the optimum values of the tuning parameters, which further determined the suitable settings which would reduce the overshooting of the intermediate body. This is the extendable part which allows the payload to move both upward and downward. The results have shown that this approach enables maintained stability within the system, as well as an improved angular position of the intermediate body [13]. A larger overshooting following the displacement of the vehicle has yet to be resolved, which could not guarantee the comfort and safety of fellow users.

With this, a combined approach of both FLCT1 and PID has further been proposed for the case of the two-wheeled

mobile robot. The system is analyzed based on the center of gravity (COG) of the mobile robot's extendable double-link, where the stability of both Link1 and Link2 is controlled using the FLCT1 approach, while the distance for the extendable link is controlled via the PID controller [11]. The input reference of Link1 is determined using COG for both with and without a mass of the payload. Given stability and performance, the objectives have been successfully achieved within the system by using this combination approach [11].

Almeshal *et al.* have taken on a different approach with a newly configured double-link two wheels machine, which accounts for the combination of PD and PID controllers in handling the system's performance under various disruptions [12]. The system derives its system through the Lagrangian approach, which consisted of a movable payload of up to 0.2m on a two-wheeled machine. The PD controller is used to control the rotation of the wheels and the angular of Link1, whereas, the PID controller is used to control the distance of the payload and the angular of Link2, respectively. Robustness of the PD-PID controller approach has been further tested with disruptions applied on both wheels, both links and the linear actuator. Herewith, findings presented have supported this approach's compatibility in handling multiple disruptions, with providing considerable stability and angular position at disruptions up to 300N. However, the system is solely tested under heuristic parameters, making the values applied in this study deviate from their optimal value. Thus, proper tuning can hereby be used in seeking more optimum values for the parameters.

Moreover, the FLCT1 approach has also been compared using a two-wheeled wheelchair with movable payload, alongside the LQR approach in both the simulation and hardware implementations [10]. This study remains in its focus to determine the approach that brings about better stability to the system in an upright position. Undoubtedly, the proposed FLCT1 approach has comparatively prevailed in providing greater stability, reducing overshoot, and shorter settling time; yet, with the scissor mechanism applied in the system's design, the height extension of the wheelchair has been limited to a mere maximum extension of 0.18m.

Aside from that, the stability of a double-link inverted pendulum system on the cart has also been extensively studied in multiple research which emphasized conventional-based controllers, including the study on the LQR approach in seeking for optimal control for system's stability [19], a comparison between the LQR and PID approaches to find the best solution for stabilization [20], a study on the swing-up control mechanism [21], as well as a look into the optimal neural network-based state-dependent Riccati equation alongside the LQR approach [23]–[25]. With these controllers being further expanded upon studies on two-wheeled robots with double-link inverted pendulum system, it is noticed that none of the researchers had reported findings on system stability through the application of Interval Type-2 Fuzzy Logic Control (IT2FLC), specifically in the area of a two-wheeled wheelchair with a movable payload.

In particular, a comparative study conducted by Castillo *et al.* between IT2FLC and FLCT1 within type-2 fuzzy inference systems have determined the former as being a more superior controller in terms of lower simulation errors (absent of noises) [40]. Another investigation conducted by Naik in assessing pitch angle of wind energy systems, under the simulated scenario of extreme wind speed disturbances, has yet again highlighted IT2FLC as the dominant approach to FLCT1 in managing system stability by maintaining factors of rotor speed, overshoot and rise time [39]. The compatibility of IT2FLC towards controlling highly nonlinear systems with a great extent of uncertainties has, thus, been justified.

The current controllers for the existing system have demonstrated limited prowess in controlling highly nonlinear systems with various uncertainties and an additional degree of freedom (DOF), thereby, proposed possible improvement areas. Whereas, the later IT2FLC, despite the capability to manage systems with great uncertainties, has yet to unveil its contributions within the mentioned system due to limited tests conducted on the investigated topic. Over the past decade, most researchers have highlighted the use of optimization methods in obtaining optimum parameters, rather than adopting the conventional method (heuristic tuning based on trial-and-error). This is due to the time-consuming, unrealistic, and unreliable factors to determine that the system is operating within its optimum parameters.

Thus, the integration of optimization approaches is preferred over conventional methods, towards acquiring optimized system parameters, and the SDA approach remains unexplored for the current controller. Besides, the performance of the two-wheeled wheelchair with movable payload can be enhanced in terms of the traveled distance, the magnitude of the angular position, and the magnitude of the torques using the optimized IT2FLC based on the SDA approaches. Therefore, an enhanced IT2FLC based SDA optimization can be a compelling area of study, specifically to improve the safety and comfort of a double-link inverted pendulum on the two-wheeled system.

The enhanced IT2FLC approach was proposed to be used for a two-wheeled wheelchair with movable payload designed using the SW4D software to further study its effectiveness as a stability controller. With this, SDA was applied to find the optimum values of certain parameters, controller gains, input control gains, and output control gains. The robustness of the proposed controller was then tested by subjecting it to various disturbances and conditions; during static motion, performing linear forward and backward motions, and moving uphill and downhill motions with the inclusion of a moving payload which accounts for an additional degree of freedom and uncertainties to the system. The system was tested with various disturbances to test the robustness in terms of the safety and comfort of the user while using the two-wheeled wheelchair in their daily activities. This was done because uncertainties were the most important issues that need to be addressed in an inverted pendulum system,

especially on high DOF systems as a wheelchair with a movable payload mechanism. In addition, the system is also tested on two different surfaces, which are flat and inclined surface to ensure the performance is at an optimal level to represent the real-world application. This is because in the real environment, the user might perform their daily routines indoors (mostly on a flat surface) as well as outdoors (including ramp surface).

This paper is organized into six sections. Section 1 introduces key issues related to the study. Section 2 describes the system model and parameters, while Section 3 presents the IT2FLC architecture. Section 4 explains the experimental setup of this study, and Section 5 reports the simulation results and discussions. Finally, this study is concluded in Section 6.

II. DESIGN OF TWO-WHEELED DOUBLE LINKS WHEELCHAIR WITH MOVABLE PAYLOAD

In this research, one of the Computer-Aided Design (CAD) software called SW4D was adopted to design a double-link inverted pendulum of a two-wheeled wheelchair. This new version of SW4D software acted as a primary replacement to the mathematical modeling before implementing it to real hardware, as it only required a shorter time-frame in deriving an accurate equation from a complex deviation [41]–[43]. Not to mention, SW4D brought about the advantage of having similar to the real system; nonlinearity, mass, gravity, and friction of a two-wheeled wheelchair within the software environment throughout this study.

The two-wheeled wheelchair examined in this study is a movable payload system, whereby its seat can be extended up to a vertical range of 0.25m, with the inclusion of a human load (approximately 70kg) when the linear actuator is activated. Besides, the design comprised of a right wheel and a left wheel operated through the independent motor on each wheel, which is connected with the bottom base. Herewith, Link1 is fixed on the center of the bottom base, while Link2 is connected to the motors. The seat of the wheelchair is further connected to the linear actuator for the purpose of height control, and the payload is attached above the seat in the form of a humanoid.

To further demonstrate the system designed for the purpose of this study, a schematic diagram of the two-wheeled wheelchair is presented in Fig. 1. As shown, the locations of the angular of Link1, the angular of Link2, the torque between Link1 and Link2, the torque on both wheels (left and right), and the linear actuator that is depicted within the diagram. The parameters of each aspect of the wheelchair have been tabulated in Table 1.

A complete model of the system designed is further illustrated in Fig. 2, with the inclusion of a concentrated force, is applied horizontally to the back of the seat, which represents the incoming simulated disturbances with a pulse signal during experimentation. Disturbances are applied in four specified conditions 1) when the seat is moving upward, 2) the seat is moving downward, 3) while the seat is extended to its maximum height, and 4) the seat without any height
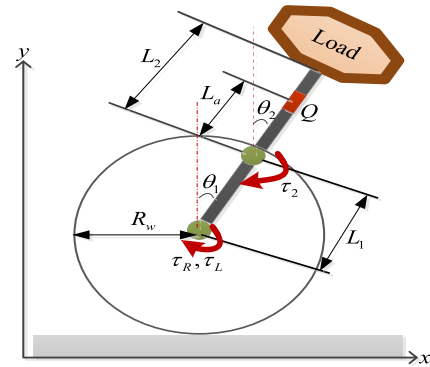

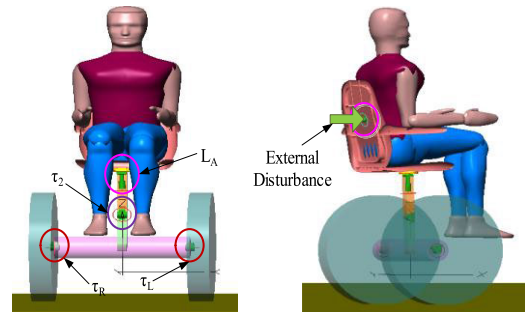**FIGURE 1.** Schematic diagram of two-wheeled wheelchair.

FIGURE 2. Complete model of two-wheeled wheelchair.

TABLE 1. Parameters of two-wheeled wheelchair.

Symbol	Description	Parameter
Θ_1	The angular position of Link1	degree
Θ_2	The angular position of Link2	degree
R_w	Radius of wheel	0.3m
τ_R, τ_L, τ_2	Torque at right/left wheel and between Link1 & Link2	Nm
L_1	Length of Link1	0.2m
L_2	Length of Link2	0.22m
Q	Displacement of the linear actuator	m
L_a	Length of the linear actuator from the upper link	m

extension. The dimensions of the system have been tabulated in Table 2.

III. DESIGN OF SDA-BASED INTERVAL TYPE-2 FUZZY LOGIC CONTROLLER

Lotfi Zadeh had first introduced IT2FLC in 1975. It became a popular approach among researchers from the year 2001 onwards, in controlling difficult and complex systems within their studies [5], [26]–[31]. In addition, the IT2FLC has also been used to control the global path planning for the mobile robot [46]. Besides, the IT2FLC has been enhanced to become the generalized IT2FLC in order to analyze the comparative study of noise robustness of IT2FLC [47]. The IT2FLC is hereby applied within highly

TABLE 2. The dimension of two-wheeled wheelchair.

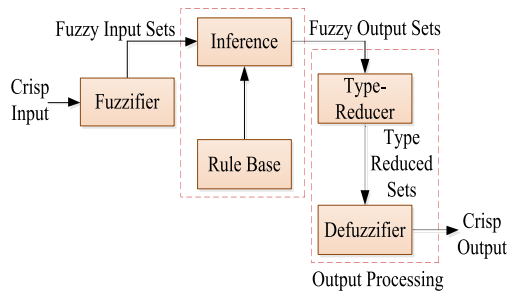| Part	Size (m)	Weight (Kg)
Wheel	Radius=0.3, Width=0.09	1.500
Axle	Radius=0.06, Length=0.55	20.00
Link1	Width=0.04, Length=0.04, Height=0.2	3.000
Link2	Width=0.04, Length=0.04, Height=0.22	3.000
Chair seat	Width=0.4, Length=0.5, Height=0.101	0.205
Back rest	Width=0.04, Length=0.04, Height=0.22	0.300
Humanoid	Height=1.75m	70.00

FIGURE 3. The architecture of Interval Type-2 Fuzzy Logic Control.

nonlinear systems like the control algorithm in handling potential nonlinearities and uncertainties that might occur in various situations. Therefore, taking into consideration the fore-mentioned conditions, IT2FLC is proposed within this study to control the stabilization of a two-wheeled wheelchair with movable payload, under the execution of the Matlab Simulink. However, before subsequent motion-based experimentation on the system can be executed, it is imperative to note that the stability of angular positions for both Link1 and Link2 in an upright position must be assured.

IT2FLC consists of five main components, namely fuzzifier, rule base, inference engine, type-reducer, and defuzzifier, as shown in Fig. 3. The rules of IT2FLC remain similar to those of FLCT1; with both the input and output of the proposed process being represented by Type-2 Fuzzy Set (T2FS), as defined by the rules of the fuzzy logic system. The fired rules are hereby combined with the inference engine to map the output T2FS from input T2FS.

With this, the IT2FLC process starts with the fuzzification of the crisp input variables (error and change of error) into the input T2FS. A singleton fuzzification is usually used within this context due to its suitability and simplicity for the embedded processor and real-time applications. This is followed by the activation of the inference engine and the rule base, which produces the output T2FS. This Type-2 fuzzy output is then processed by the type reducer; specifically, with the adoption of the Nie-Tan method for the type-reduction process within this study. Once the type-reduction process is completed, the crisp output is obtained by having the approximate type-reduced sets defuzzified and sent to the actuators. A T2FS $\tilde{A}$ is defined as in (1).

$$
\begin{aligned}
\tilde{A} &= \int_{x \in X} \int_{u \in J_x} \mu_{\tilde{A}}(x, u)/(x, u), \quad where \ J_x \in [0, 1] \\
\tilde{A} &= \int_{x \in X} \left[\int_{u \in J_x} f_x(u)/u \right]/x, \quad where \ J_x \in [0, 1] \\
\tilde{A} &= \int_{x \in X} \left[\int_{u \in J_x} 1/u \right]/x, \quad where \ J_x \in [0, 1] \\
\tilde{A} &= \int_{x \in X} \left[\int_{u \in J_x} 1/u \right]/x, \quad where \ J_x \in [0, 1]
\end{aligned} \tag{1}
$$

where, to denote, the union is the overall admissible input variables x and u; x represents the primary variable $x \in X$; u represents the secondary variable, $u \in U$; $J_x \in [0, 1]$ represents the primary membership of x; $\mu_{\tilde{A}}(x, u)$ represents T1FS, also known as the secondary set; with the secondary grades of $\tilde{A}$ being determined as $f_x(u) = 1$. The union of all the primary memberships for a T2FS, $\tilde{A}$ is known as the footprint of uncertainty (FOU) of $\tilde{A}$, whereby FOU is a key concept of T2FS, which models the uncertainties within the position and shape of the fuzzy set [15]. The primary membership of x, J_x is defined as in (2).

$$
J_x = \left\{ (x, u) : u \in [\underline{\mu}_{\tilde{A}}(x), \bar{\mu}_{\tilde{A}}(x)] \right\} \tag{2}
$$

The FOU of $\tilde{A}$ is defined as in (3).

$$
FOU\left(\tilde{A}\right) = \bigcup_{\forall x \in X} J_x = \{(x, u) : u \in J_x \in [0, 1]\} \tag{3}
$$

Essentially, the FOU of $\tilde{A}$ is bounded by two membership functions (MFs) of Type-1, known as the upper membership function (UMF) and the lower membership function (LMF) of $\tilde{A}$, as presented in Fig. 4. For FOU $(\tilde{A})$, it's upper bound (UMF) is denoted by $\bar{\mu}_{\tilde{A}}(x)$, $\forall x \in X$, while its lower bound (LMF) is denoted by $\bar{\mu}_{\tilde{A}}(x) = \overline{FOU(\tilde{A})} \forall x \in X$ [15]. The UMF is defined as in (4).

$$
\bar{\mu}_{\tilde{A}}(x) = \overline{FOU(\tilde{A})} \quad \forall x \in X \tag{4}
$$

The LMF is defined as in (5).

$$
\underline{\mu}_{\tilde{A}}(x) = \underline{FOU(\tilde{A})} \quad \forall x \in X \tag{5}
$$

There are several methods of type-reduction that can be applied to T2FS, including the Karnik-Mendel method [32], the Enhanced Karnik-Mendel method [33], the Wu-Mendel Uncertainty Bound method [34], the Nie-Tan method [15], the Bagain-Melek-Mendel method [35], the Iterative Algorithm with Stop Condition [36], [37] and the Enhanced Iterative Algorithm with Stop Condition [38].

As previously mentioned, the Nie-Tan method has been specifically applied to the current study as it can simultaneously fulfill both the steps of the type-reduction and defuzzification within the IT2FLC process [16]. As such, the Nie-Tan method is defined as (6).

$$
y_i = \frac{\sum_{n=1}^{N} b_k \left(\overline{\mu}_{\tilde{A}^i}(x) + \underline{\mu}_{\tilde{A}^i}(x) \right)}{\sum_{n=1}^{N} \left(\overline{\mu}_{\tilde{A}^i}(x) + \underline{\mu}_{\tilde{A}^i}(x) \right)} \tag{6}
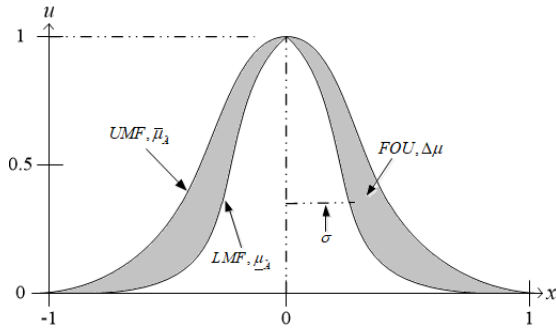$$

FIGURE 4. Interval Type-2 Fuzzy Set.

where b_k is the centers of the output MFs, $\overline{\mu}_{\tilde{A}^i}(x)$ is the upper membership grades of $\tilde{A}^i(x)$, and $\underline{\mu}_{\tilde{A}^i}(x)$ is the lower membership grades of $\tilde{A}^i(x)$.

For this paper, various disturbances from the force of $\pm 100N$ up to the force of $\pm 1000N$ are applied to the developed model in the SW4D software, with an upward and downward motion of seat in several conditions. The vertical motions of the payload are operated via a linear actuator, which increases the sensitivity as well as DOF, complexity, and nonlinearity of the system. Furthermore, a total of five MFs of error, change of error and output have been defined to achieve the goals of the system, namely Negative Big (NB), Negative Small (NS), Zero (Z), Positive Small (PS) and Positive Big (PB).

Several types of MFs in T2FS have been noted: namely, the Trapezoidal, Gaussian, and Triangle shaped MFs. The Gaussian shape is used in this study, in its MFs for all the inputs and outputs as it is simpler in design as well as being easier to be represented and optimized. Besides, the Gaussian-shaped MFs require a shorter time to be computed for smaller rule bases, yet it produces good and smooth output results and steady responses of the two-wheeled wheelchair system compared to the other shapes. As shown in Fig. 4, which illustrates T2FS with a boundary, the five Gaussian MFs for each input and output used in this paper possess the parameters of uncertain means, $\Delta\mu$ and standard deviation, σ that need to be optimized to get the system's optimal values. With the positions of the input MFs fixed between -1 and $+1$, the standard values of $\Delta\mu$ and σ have been recorded at 0.125 and 0.418 respectively.

Moreover, the Mamdani inference is determined as a good option to be utilized within this paper, as it is easily understood, and its rules can be simply formulated, especially with limitations of the available information regarding the system [8]. Table 3 presents the MFs with five levels of each input and output, with 25 rules comprising the errors for the angular positions, e_i and the change of error for angular positions, Δe_j of Link1 and Link2. The IF-THEN rule is further applied to construct the system's rule base, as follows:

If e_i is NB and Δe_j is NB, then u is PB

If e_i is NB and Δe_j is NS, then u is PB

TABLE 3. Rules of interval type-2 fuzzy logic control.

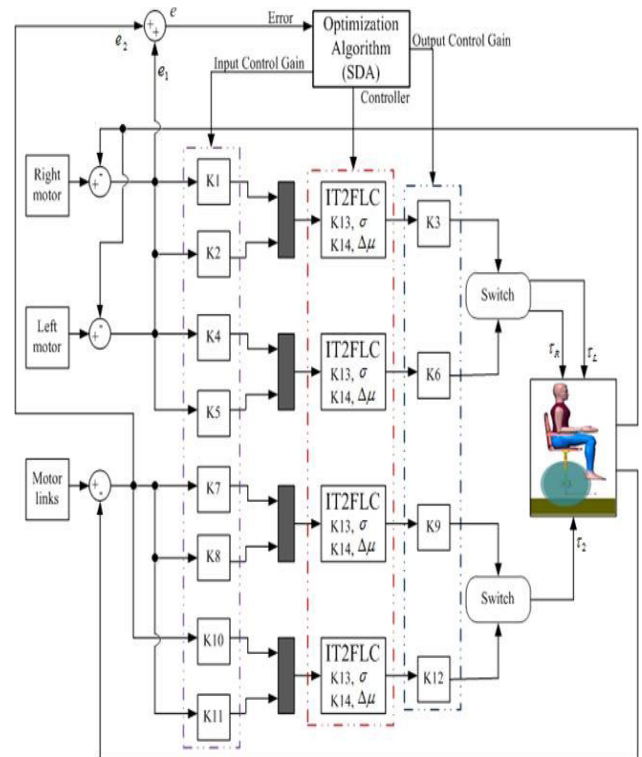| e/Δe	NB	NS	Z	PS	PB
NB	PB	PB	PB	PS	Z
NS	PB	PB	PS	Z	NS
Z	PB	PS	Z	NS	NB
PS	PS	Z	NS	NB	NB
PB	Z	NS	NB	NB	NB

FIGURE 5. Integration of developed model for the system (between SDA-IT2FLC, and SW4D).

If e_i is NB and Δe_j is Z, then u is PB

If e_i is NB and Δe_j is NS, then u is PS

If e_i is NB and Δe_j is PB, then u is Z

For control purposes, the developed two-wheeled wheelchair system with movable payload in the SW4D environment would need to be integrated with SDA-IT2FLC, as shown in Fig. 5. This is enabled by identifying the developed system in SW4D as a based plant, which is then merged with the Matlab/Simulink, by installing SW4D into Simulink's toolbox environment. There are two loops of the controller of IT2FLC, which have been designed to control the stabilization of the system, with each loop consists of four input gains and two output gains.

Fig. 5 illustrates the locations of the input control gains, output control gains, and the controller's membership in which the optimum parameters would be determined, with $\Delta\mu$ being the blurred area of uncertainties in IT2FLC and σ being the width of the Gaussian MFs.

Herewith, the control input gains and the output gains are used to control the input spread of the MFs and the spread of

output MFs, respectively. Following all the input/output gains that require optimization to obtain the optimal value of each gain, a total of 14 parameters would have to be optimized using the SDA; eight parameters for the input gains, four parameters for the output gains and controller's membership ($\Delta\mu$ and σ).

The dynamic mathematical formula for the spiral radius of SDA is hereby defined as in (7) [44].

$$x_i(k+1) = S_n(r,\theta)x_i(k) - [S_n(r,\theta) - I_n]x^*$$
$$S_n = rR^n \tag{7}$$

where, $i=1,2,3,\dots,m$, x represents a coordinate location of the point, k represents the number of iteration, θ represents the angle or displacement, r represents the spiral radius or convergence rate, x^* represents the center point of the spiral, S_n represents the multiplication of radius, and R^n represents the composition of the rotational matrix.

In this work, the parameters of SDA, $r=0.99$, and $\theta = \pi/4$ are used as the shape of a spiral dynamic trajectory, where 50 search agents and 50 iterations are used. The Root Mean Square Error (RMSE) has been chosen as an objective function in this paper, with its formula being defined as in (8).

$$RMSE = \sqrt{\frac{1}{N}\sum_{1=1}^{N} e_i^2} \tag{8}$$
$$e_i = \theta_{desired} - \theta_{actual} \tag{9}$$

where, $i=1,2,\dots,N$, e_i is the error of an angular position, $\theta_{desired}$ represents the desired angular position, and θ_{actual} represents the actual angular position.

The single objective function, F is given as the summation of RMSE function for this study, by taking the weighted sum of errors. The purpose of the SDA's objective function is to minimize the error of angular positions of Link1 and Link2 when the system stabilizes both angles of Link1 and Link2 to ensure the stabilization of the two-wheeled wheelchair in an upright position. The single objective function is defined as in (10).

$$F = w_1 RMSE_1 + w_2 RMSE_2 \tag{10}$$

where $RMSE_1$ is the error of the angular position of Link1, $RMSE_2$ is the error of the angular position of Link2, w_1 is the weighted sum for error$_1$, and w_2 is the weighted sum for error$_2$. The weight vector of this system is $[w_1\ w_2] = [0.7\ 0.3]$. Noted that w_1 is weighted larger than w_2 because the angular position of Link1 in this system is crucial to create stability compared to the angular position of Link2.

From the beginning, stabilization has always been the utmost important aspect of the system in this paper. Therefore, more effort is required IT2FLC controller to ensure the competency of the two-wheeled wheelchair with movable payload to maintain stability in an upright position while performing various tasks. In achieving this objective, Fig. 6 outlined the switching mechanism for the stabilization of the system's links. The schematic diagram of the switching mechanism would have a high gain and low gain in output
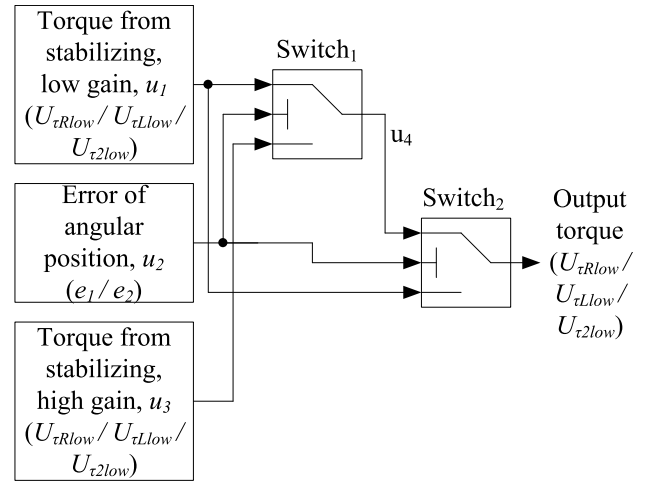

FIGURE 6. Switching mechanism for the stabilization of the system.

scaling parameters that are affected by stabilization of the system, which consisted of u_1 for the first input, u_2 for threshold, and u_3 for the second input.

The switch will only be activated when the error of angular position is within a small range. For the case of a two-wheeled wheelchair system with movable payload, the range towards activation has been decided within $\pm 3°$ thresholds for Switch1 and Switch2 are set to have the higher limit of $+3°$ and low limit of $-3°$, as accordingly. The switch shall be executed where the second input, $u_{3,}$ meets the requirement or the first input, u_1 whenever the value $\geq$ threshold, u_2.

The condition of the switching mechanism is defined in (11) with the location of the notation being illustrated in Fig. 6.

$$U_{\tau R} = \begin{cases} y_i * u_{\tau Rlow}, & -3° \leq \theta_1 \leq 3° \\ y_i * u_{\tau Rhigh}, & otherwise \end{cases}$$
$$U_{\tau L} = \begin{cases} y_i * u_{\tau Llow}, & -3° \leq \theta_1 \leq 3° \\ y_i * u_{\tau Lhigh}, & otherwise \end{cases}$$
$$U_{\tau 2} = \begin{cases} y_i * u_{\tau 2low}, & -3° \leq \theta_2 \leq 3° \\ y_i * u_{\tau high}, & otherwise \end{cases} \tag{11}$$

where y_i represents the output from the controller as express in (6) with $i=1,2,3\dots m$, $U\tau_R$, and $U\tau_L$ represent torque at the right and left wheels; $U\tau_2$ represents the torque between Link1 and Link2; $u_{\tau Rlow}$ and $u_{\tau Rhigh}$ represent the low and high gain for torque at the right wheel; $u_{\tau Llow}$ and $u_{\tau Lhigh}$ represent the low and high gain for torque at the left wheel; $u_{\tau 2low}$ and $u_{\tau 2high}$ represent the low and high gain for the torque between Link1 and Link2.

IV. EXPERIMENTAL SETUP
In this paper, the experiments were simulated via the use of enhanced IT2FLC, in which the parameters of the main control IT2FLC parameters, $\Delta\mu$ and σ as well as input and output control gains, were optimized through the SDA
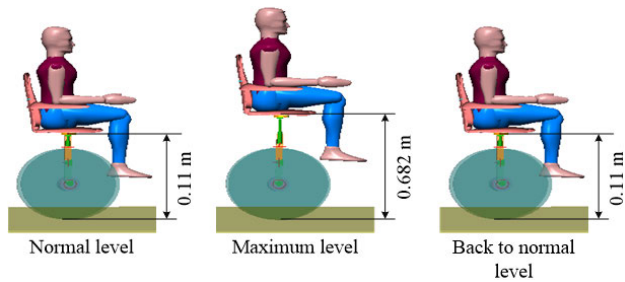
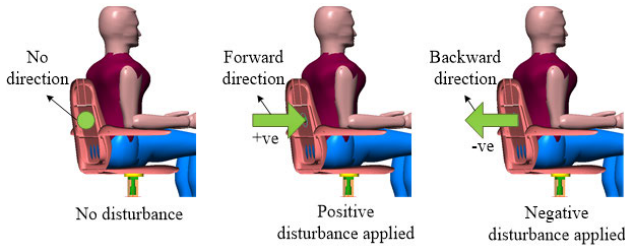**FIGURE 7.** Height extension transformation of two-wheeled wheelchair.

FIGURE 8. Direction of the positive and negative disturbance.

TABLE 4. Extension of seat and external disturbance.

Experiment	Time (s)	Height of seat	Force (N)
1st experiment	05.0	Normal level	+100
	15.0	Maximum level	-100
	25.0	Maximum level	+150
	35.0	Normal level	-150
	45.0	Normal level	+200
	55.0	Maximum level	-200
	65.0	Maximum level	+250
	75.0	Normal level	-250
	85.0	Normal level	+300
	95.0	Maximum level	-300
	105.0	Maximum level	+350
2nd experiment	15.0	Maximum level	+1000
	35.0	Normal level	-1000
	60.5	Moving down	-1000
	80.5	Moving up	+1000
3rd experiment	15.0	Maximum level	+1000
	35.0	Normal level	-1000
	60.5	Moving down	-1000
	80.5	Moving up	+1000
4th experiment	10.0	Maximum level	+500
	20.0	Normal level	-500
	30.0	Maximum level	-500
	40.0	Normal level	+500
5th experiment	10.0	Maximum level	+300
	20.0	Normal level	-300
	30.0	Maximum level	-300
	40.0	Normal level	+300

(SDA-IT2FLC). In particular, five key experiments were conducted to investigate the robustness of the SDA-IT2FLC for the developed model, with the first experiment that examined the performance while the system was in the static condition; the next experiments tested the system while performing moving forward and backward motion control; and the last experiments which tested the system while performing a moving uphill and downhill motion control. In addition, the entire experiments that were conducted in this paper, while external disturbance forces were applied to the system at the back of the seat and the moving payload at the same time.

Table 4 further shows the time intervals in which external disturbances are applied, the condition for the height of the seat of the two-wheeled wheelchair, and the magnitude of external disturbances applied to the back of the seat. The vertical extraction and retraction motions of the seat's height for the developed system are presented in Fig. 7. Particularly for this study, the transformation in the seat's height extends from 0.11m up to 0.25m at its maximum, while being able to retract back to its previous height in carrying out the experiments. Fig. 8 illustrates the directions of the external disturbance force applied to the back of the seat during the experiments, whereby a positive force is a disturbance applied in the forward direction and vice versa.

Fig. 9 and Fig. 10 illustrate the two-wheeled wheelchair while performing forward and backward motion controls between two independent locations (Point A and Point B) on a flat surface. While the illustration of the system while performing moving uphill and downhill from Point A to Point B can be seen in Fig. 11, and Fig. 12 respectively.

V. RESULTS AND DISCUSSION
A. OPTIMIZED PARAMETERS
As mentioned in the previous section, 14 parameters would require optimization to improve the stability, as well as
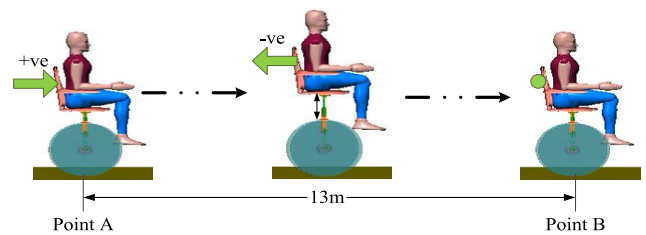

FIGURE 9. Two-wheeled wheelchair performing moving forward.

mobility of the developed system, which consisted of eight parameters for input control gains, four parameters for output control gains, and two main parameters for the controller's membership ($\Delta\mu$ and σ). As presented in Table 5, the input and output control gains adopted the lowest and highest gain values. Based on the fact that the controllers were analyzed within the current study, different parameters for IT2FLC (based on heuristic tuning), and SDA-IT2FLC are described in Table 5, which would be used to stabilize the two-wheeled wheelchair system in performing the designated tasks.
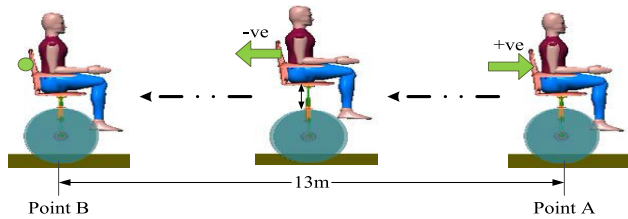
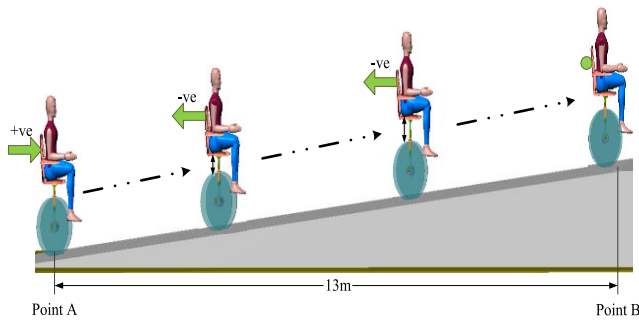**FIGURE 10.** Two-wheeled wheelchair performing moving backward.

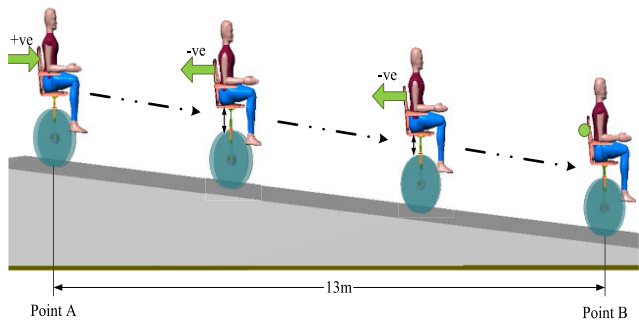**FIGURE 11.** Two-wheeled wheelchair performing moving uphill.

FIGURE 12. Two-wheeled wheelchair performing moving downhill.

A comparison between the proposed SDA-IT2FLC, IT2FLC, and FLCT1 (used in the previous design) is conducted following the first experiment when the developed system was in a static position. With excellent performance demonstrated by the proposed controller on the system stability over its predecessors, subsequent experiments were only simulated through optimized parameters, solely on SDA-IT2FLC, towards verifying the controller's robustness in handling a multitude of other situations.

B. PERFORMANCE OF SYSTEM IN STATIC CONDITION WITH VARIOUS FORCES OF DISTURBANCE REJECTION

As conducted in previous work [6], [9], the robustness of IT2FLC was verified against the earlier FLCT1, in which identical disturbance patterns had been applied in creating similar uncertain conditions. IT2FLC had seemingly overshadowed the fore-analyzed FLCT1 in terms of stability control of a two-wheeled wheelchair system; this experiment considered simulation towards comparing heuristic and SDA-based IT2FLC. In particular, performance following

TABLE 5. Parameters of gain using SDA.

Gains	Parameters	SDA-IT2FLC
K1	Input control gain	0.8024
K2	Input control gain	0.3538
K3	Output control gain	99.660
K4	Input control gain	3.7553
K5	Input control gain	0.0980
K6	Output control gain	53.344
K7	Input control gain	1.0500
K8	Input control gain	0.5366
K9	Output control gain	-205.0
K10	Input control gain	7.2138
K11	Input control gain	0.3918
K12	Output control gain	-105.0
K13	Delta	0.0500
K14	Sigma	0.3600

control parameters of the proposed approach would then be placed in comparison with the results from the earlier design (FLCT1 based system), to further support findings for this experiment. The purpose of the experiment in static condition with disturbance rejection was to represent the two-wheeled wheelchair system is a stationary condition, i.e., watching television or having a conversation with other people in the indoor and outdoor environments. This is because the user needs to remain static in one place for a long time without moving.

Fig. 13 shows the performance of the system within a 120s timeframe, with forces of varying directions (positive and negative) and magnitude, consisted of ±100N, ±300N, and $+350$N, would be exerted while having simultaneous payload motions (upward and downward movements) of up to 0.25m following a 10s interval. Considering the pre-set scenario, the simulation is reckoned to cause tilting of the two-wheeled wheelchair system upon directions of the forces, where positive and negative forces would cause forward and backward tilting, respectively.

While the system is statically positioned, a traveled distance of about 0.003m has been recorded for both approaches of IT2FLC and SDA-IT2FLC throughout the simulated timeframe despite varying external disturbances, which is deemed minimal and negligible for the current case. Moreover, recorded torque for the left and right wheels, as well as the torque between Link1 and Link2, has also been presented. Spotlight is shined upon maximum torque for both IT2FLC and SDA-IT2FLC, determined to be <3Nm at the right wheel, <5Nm at the left wheel, and <4Nm between Link1 and Link2. However, the shortfall has been displayed with a relatively high initial torque of 6Nm at the left wheel when IT2FLC is implemented.

The angular positions, being a direct representation of the system's fluctuation in influencing users' comfort when

TABLE 6. Performance comparison between SDA-IT2FLC and FLCT1.

Aspect / Author	N. F. Jamin (currently proposed controller)	S. Ahmad, 2011, 2014
System	Two-wheeled wheelchair with a movable payload	Four-wheeled to a two-wheeled wheelchair
Controller	SDA-IT2FLC	FLCT1
Settling time after disturbed, (s)	<5	<5
Traveled distance, (m)	0.006	12
Peak angle amplitude of Link1 after disturbed, (degree)	<±1.1	<5
Peak angle amplitude of Link2 after disturbed, (degree)	<±0.55	<2
Peak torque right wheel after disturbed, (Nm)	<±3.5	>±50
Peak torque left wheel after disturbed, (Nm)	<±4.5	>±50
Peak torque between L1L2 after disturbed, (Nm)	<±4	>±50

TABLE 7. Performance comparison between IT2FLC and SDA-IT2FLC of the various forces system control.

Aspect / Controller	Settling time after disturbance, (s)		Peak overshoot, (degree), (Nm)		Peak undershoot, (degree), (Nm)	
	IT2FLC	SDA-IT2FLC	IT2FLC	SDA-IT2FLC	IT2FLC	SDA-IT2FLC
Link1, θ_1	-	5.34	0.7264	0.5412	-1.5390	-1.0310
Link2, θ_2	-	5.00	0.4068	0.3009	-0.3992	-0.1979
Torque right wheel, τ_R	6.00	6.00	1.8540	1.8540	-3.4780	-3.4780
Torque left wheel, τ_L	5.00	5.00	6.5500	6.5500	-4.3410	-4.3410
Torque between L1L2, τ_2	6.00	6.00	2.6150	2.6150	-3.8800	-3.8800

operating the wheelchair, would then play a more prominent role in assessing the analyzed controllers. The angular positions of Link1 and Link2 can be seen in Fig. 13. Graphical descriptions have established SDA-IT2FLC as a more effective approach towards a system and Link2, respectively. However, IT2FLC which significantly paled in comparison to the optimized performance compared to its heuristic counterpart, with the angular positions below ±1° and ±0.4° for Link1 controller in the angular positions, has demonstrated commendable results over FLCT1, denoting a 68% and 77% reduction in angular positions of Link1 and Link2 to the previous design [6], [9].

The entirety of results obtained following simulation based on the pre-set situation for the current experiment has been outlined in Table 6, which placed a straight comparison between IT2FLC and SDA-IT2FLC in the aspects of resolving time, peak overshoot and peak undershoot. Assessed upon these dimensions have also weighted the later SDA-IT2FLC for better fluctuation management against IT2FLC. With mere ±3N in torque at both links as recorded for SDA-IT2FLC, it is worth mentioning that the previously implemented FLCT1 has produced larger torque of up to ±50N with ensuing influences by external disturbances under identical magnitude; which denotes a 94% reduction in the value of torque on both links, further fluctuation. Further reviews in Table 7 reveals a 98.5% reduction in the traveled distance that has been acknowledged through the proposed controller SDA-IT2FLC over FLCT1, although an earlier design had excluded the complexity of movable payload mechanism. Therefore, SDA-IT2FLC is proven to enable better stability performance while handing highly nonlinear systems with greater complexity.

In this experiment, the previous FLCT1 has been overshadowed by IT2FLC, more so when optimum parameters are obtained through the application of SDA optimization. Therefore, the stability has been placed on findings

in which SDA-IT2FLC would potentially be a compatible control approach for systems with heightened nonlinearity and uncertainties, specifically in ensuring the comfort and safety of the two-wheeled wheelchair users with extendable seat. Regardless, further experiments would need to be conducted to investigate the required robustness in handling the system stability under moving conditions (in-motions). Thus, the next and onwards experiment was only conducted using optimized parameters, which were the SDA-IT2FLC.

The system's performance of the proposed controller in this paper has also been compared with the performance obtained in a study by Chang et al. [45]. They focused on the design of the output feedback $H\infty$ controller to control the inverted pendulum nonlinear system based on the Takagi-Sugeno fuzzy model. As can be observed in their study, the performance of the initial angular position is about 0.7°, while the initial magnitude of the torque is between 22Nm and −14Nm. In this paper, the enhanced SDA-IT2FLC produced a very small angular position with < 0.1° at the time before being exposed to external disturbances, even though the system is a double-link inverted pendulum. Moreover, the initial magnitude of the torque is less than 1Nm without external disturbances using the SDA-IT2FLC. In addition, the system in [45] used a single-link inverted pendulum system, which has less DOF and less complexity. It is also worth mentioning that the proposed SDA-IT2FLC provides better performance compared to [45] in terms of the angular position and torque.

C. PERFORMANCE OF SYSTEM FOR MOVING FORWARD MOTION CONTROL WITH POSITIVE AND NEGATIVE FORCES DISTURBANCE REJECTION

The 2nd experiment analyzed the ability of the proposed controller in stabilizing the developed two-wheeled wheelchair system with movable payload while it was concurrently influenced by external disturbances while having forward motions on a flat surface. The previous experiment has thoroughly investigated the system's performance through the implementations of SDA-IT2FLC and its preceding controllers (heuristic IT2FLC and FLCT1) when the developed system
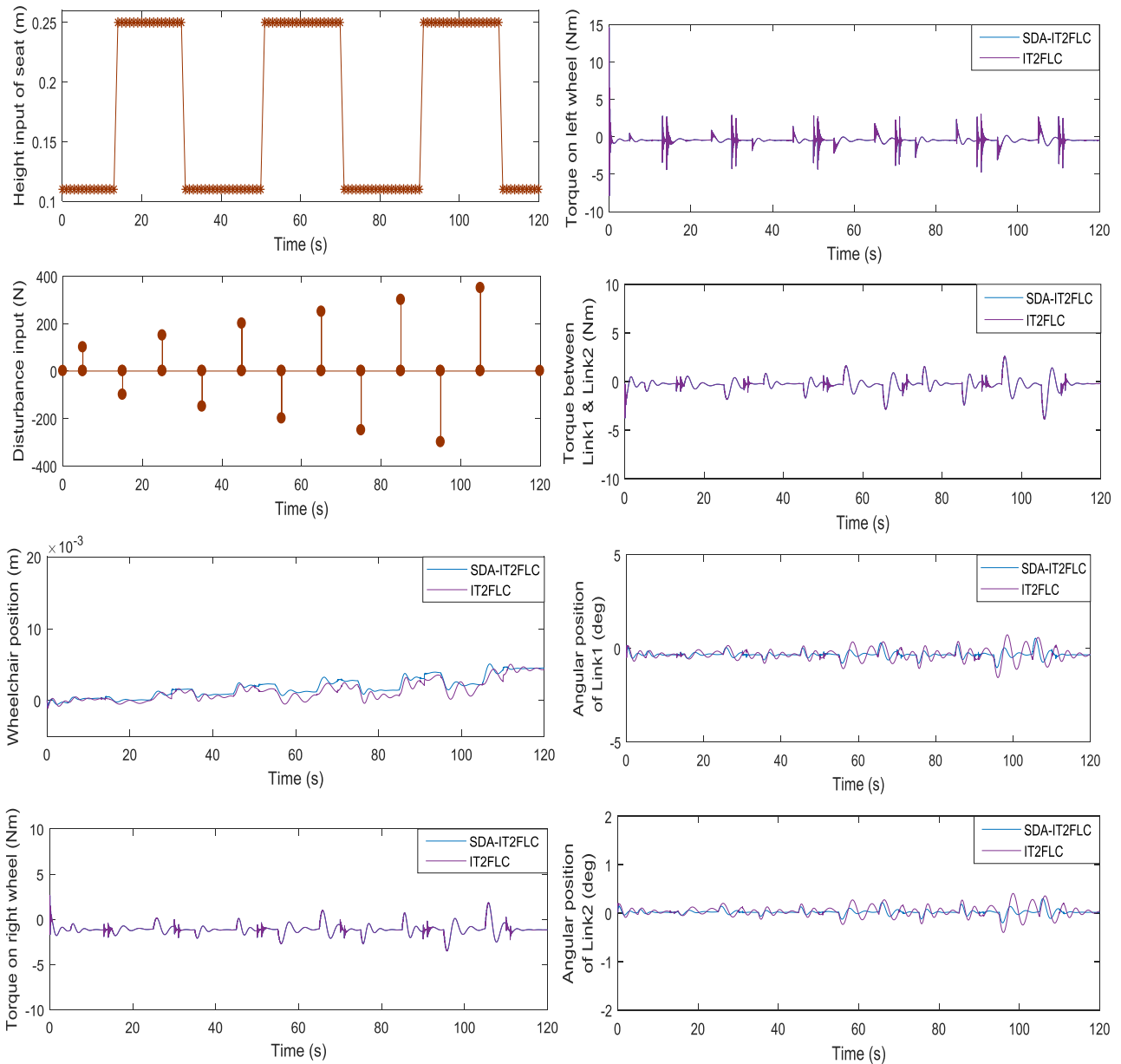
FIGURE 13. Performance of the system with various forces system control.

remained in a static condition. With SDA-IT2FLC revealed as the superior control approach, the current set would evaluate its effectiveness for more complex situations in which the developed system was being stirred in the forward direction. The purpose of this forward and backward motion control with disturbance rejection experiment is to replicate the users' use of a two-wheeled wheelchair while performing their daily basic activities indoor and outdoor, such as moving from one place to another for cooking, cleaning or even shopping, similar to a normal person. Moreover, the external disturbance force can represent the dynamic changes in the wheelchair's direction or when the wheelchair travels on the non-smooth surface such as gravel, sand, and tar pavement road.

Capitalizing solely on assessing the robustness of the SDA-IT2FLC, experiments were conducted as per the

fore-mentioned circumstance, forward motions with a combination of both positive and negative external disturbances. The objective is placed on generating a stable performance by maintaining the two-wheeled system in an upright position through withstanding the oncoming uncertainties (moving payload, linear motions on a flat surface, and external disturbance rejection). The values of the input-output gains were assessed to determine to control torque towards actuating the motors with the intention to widen the controller's parameters towards system stabilization.

In order to test the robustness of the controller in the moving forward motion control of a two-wheeled wheelchair with movable payload, the external disturbances used are in the form of pulses with ±1000N applied to the back of the seat. While the height input of the seat varied from the
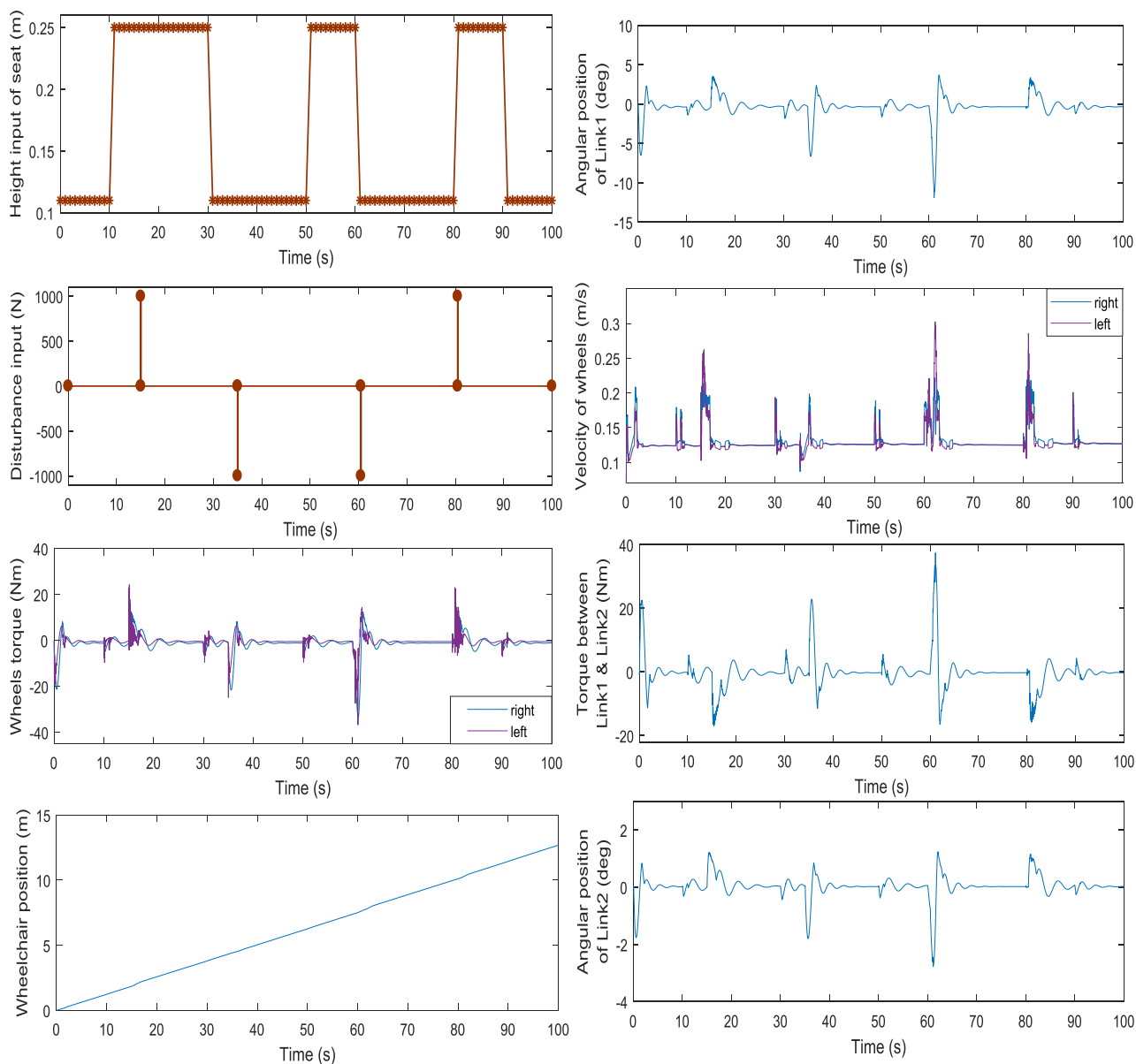
FIGURE 14. Performance of the system while moving forward motion control.

normal level to the maximum level, which is from 0.11m up to 0.25m. The system's response to the moving forward motion control can be assessed in Fig. 14. Based on findings obtained, the two-wheeled wheelchair system has traveled up to 13m throughout the simulated timeframe. Despite the different disturbance patterns, the system had maintained a slightly consistent traveled distance, with the inclusion of a movable payload, following an average velocity of 0.15m/s.

Compared to simulations where disturbances are applied from a single direction, the system's torque for both wheels and in between Link1 and Link2, have denoted a higher torque, particularly at the 60.5s of the simulated timeframe, with a value of ±40Nm. This happens when a negative force of −1000N is applied while the extended payload has

reached its maximum height of 0.25m. Such information is highlighted, like other points in which disturbances are applied had merely yielded the torque of < ±25Nm. Not to mention, performance in angular positions of Link1 and Link2 has determined comparatively higher values during the 15s and 60.5s, when negative disturbances are applied, over the recorded < 5° for points of other disturbances.

The conditions of the payload being dissimilar for both points, greater difficulties are encountered in controlling the forward-moving system when negative forces are involved, with the recorded angular positions of 5° and 2°, and 10° and 3° for Link1 and Link2, during both simulated points, respectively. With this, the developed two-wheeled wheelchair system using SDA-IT2FLC was able to settle within a short

interval upon being disturbed from multiple directions; yet, attention should be given to greater fluctuations caused by contrasted disturbance-motion directions, particularly during the process of payload elevation.

On the whole, the current set of experiments has confirmed that SDA-IT2FLC has the ability to stabilize highly nonlinear systems with the like of a two-wheeled during forward steering movement by withstanding diverging external disturbances of up to $\pm 1000N$, with the inclusion of a moving payload at the same time. Within a 100s timeframe, the proposed controller manages to retain the system's stability in an upright position while establishing linear forward motions, which in practicality would prove to be helpful among users, especially with possible incoming uncertainties from unexpected circumstances. This is also to ensure the safety and the comfort of the user while using a wheelchair without any doubt.

D. PERFORMANCE OF SYSTEM FOR MOVING BACKWARD MOTION CONTROL WITH POSITIVE AND NEGATIVE FORCES DISTURBANCE REJECTION

From a distinct point of view as the previous experiment, the 3rd experiment takes into consideration the effectiveness of SDA-IT2FLC in handling external disturbances while the system was having backward motions with the equipped movable payload on a flat surface. In this experiment, the uncertainties regarding the combination of both positive and negative disturbances on a backward stirring two-wheeled wheelchair system with movable payload are studied to assess the robustness of SDA-IT2FLC. Under a force of $\pm 1000N$ from both pro and opposed direction of the moving system, external disturbances were applied to the back of the seat, while having height input of the payload following previous simulations to create the four main conditions at the 15s, 35s, 60.5s and 80.5s across a 100s timeframe as shown in Fig. 15.

The performance of the system while doing a moving backward motion control can be seen in Fig. 15, including the traveled distance, velocity, torque for both wheels, and the torque between Link1 and Link2, as well as the angular position of Link1 and Link2. Throughout the simulated timeframe of 100s, the system had traveled up to 13m with the given velocity of -0.15m/s, following heightened stability in handling moving payload and rejecting disturbances, even when minor fluctuations can be seen between the 15s and the 60.5s. The situation in which uncertainties are coming from diverging directions would cause the system to tilt in alignment, which would differ upon the positions of the payload, and the system's motions.

Furthermore, the magnitude of the torque and angular positions obtained following the disturbance pattern, as shown in Fig. 15 indicates significant differences in terms of amplitude angles and torque for both links, in a disparity between positive and negative applications of external forces. Considering positive disturbances were applied, forces which contradicted the motion direction of the system had caused risen torque values on both wheels, as recorded at +30Nm for the 15s and

80.5s. Conversely, negative disturbances which are aligned to its motions had generated a mere −15Nm on the 35s and 60.5s, which in turn, is relatively lower. Such has also been the case for both the system's links, with a recorded value of −32Nm on positive disturbances, and < +20Nm on negative ones.

While in terms of angular positions, values of 10° and 7° have been recorded for the system's Link1 following positive disturbances, and about 4° when negative disturbances are applied. The values of < 3° and −1° are also obtained for the Link2 in a similar context. Positive disturbances have yet again shown to generate greater fluctuations in the system's stability over negative ones in this dimension. Regardless, SDA-IT2FLC remained capable of maintaining the stability of a two-wheeled wheelchair system while stirring backward on a uniform surface, withstanding movable payload and disturbance rejection from diverging directions.

Nevertheless, through the current experiment, it can be seen that the proposed SDA-IT2FLC has successfully maintained the upright stability of a two-wheeled wheelchair system with movable payload under circumstances of backward stirring, moving humanoid payload, as well as external forces with a magnitude of up to $\pm 1000N$. Herewith, a system implemented with the proposed controller has been proven viable in maneuvering across uniform surfaces, while faced with uncertainties of being unexpectedly disturbed. Despite the differences, it manages to preserve increased flexibility in greater vertical outreach. The proposed SDA-IT2FLC can ensure good stability in the upright position with less fluctuation. Thus, it can be said that the SDA-IT2FLC can protect the user from any risk or falling and simultaneously comforts the user.

E. PERFORMANCE OF SYSTEM FOR MOVING UPHILL MOTION CONTROL WITH POSITIVE AND NEGATIVE FORCES DISTURBANCE REJECTION

Following the completion of experimentation with system maneuvers over a flat surface, experiments are then conducted to control the two-wheeled wheelchair with disturbance rejection while executing uphill motions at a velocity of 0.21m/s. The velocity of the system is increased because it needs high velocity to move on an inclined surface compared to a flat surface. The control objective, in this case, was to confirm that the proposed controller, SDA-IT2FLC, worked superbly while handling a two-wheeled wheelchair system with a movable payload on an inclined surface, particularly at the uphill direction. With considerable stability, the system has demonstrated in the previous experiment, the robustness of the proposed controller is then tested with a combination of positive and negative disturbances in the form of pulses applied at a 10s repetitive gaps across the pre-set 47s timeframe, towards observing the capability of SDA-IT2FLC in handling cases of uncertainties during incline motions in an uphill direction.

The purpose of the experiment to account for the moving uphill and downhill motion control with disturbance rejection
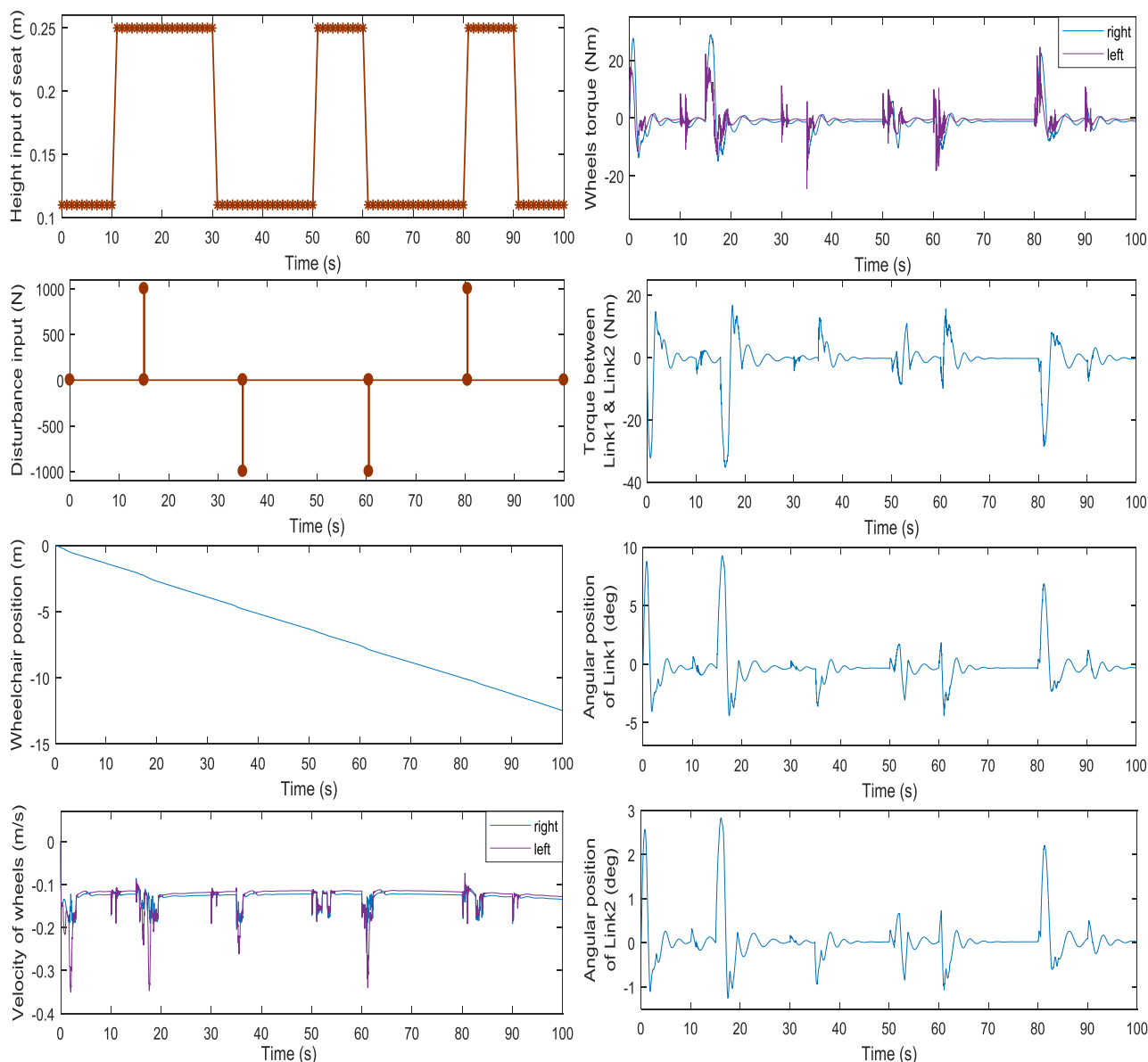
FIGURE 15. Performance of the system while moving backward motion control.

is to emulate a user when using a two-wheeled wheelchair while going out to perform any outdoor activities. The users might want to use any ramp while using a wheelchair and the external disturbance force to represent an uneven surface, and any disruptions occurred. The direction of forces applied can be seen in Fig. 16; the two-wheeled wheelchair system is disturbed with disturbances at a magnitude of ±500N to the back of its seat during two separate conditions on the height of the moving payload, at the normal level and the maximum level. The magnitude of the external disturbances was reduced from the previous experiments because the system found it difficult to handle a higher disturbance force compared to the flat surface.

There are four key moments throughout the simulation 1) the10s when the payload is elevated to its maximum level

of height, 2) the 20s when the payload is maintained without extension (normal level), 3) the 30s when the payload is elevated to its maximum level of height while being maneuvered across a higher slope and 4) the 40s when the payload is maintained without extension (normal level) near the peak of the slope. Realized lower magnitude of disturbances were applied within the current experiment to account for difficulties for the uphill maneuver at the expense of capability to handle higher external forces.

The 4th experiment was conducted to assess system performance based on the proposed controller during uphill motions while having to face simultaneous positive and negative disturbance rejection and moving payload at the same time of up to 0.2m (maximum level of the height of seat). Fig. 16 presents the findings regarding the system's performance
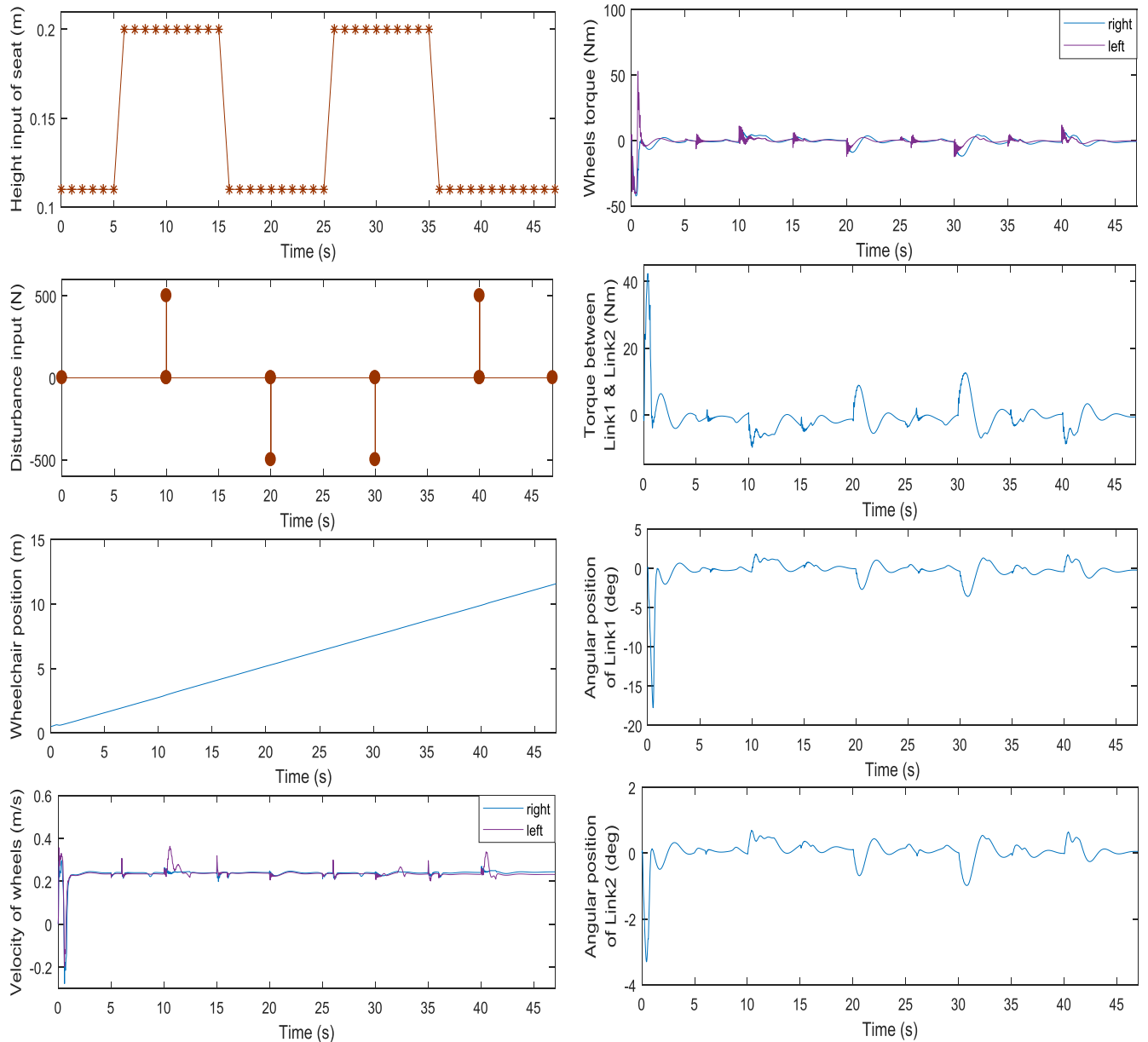
FIGURE 16. Performance of the system while moving uphill motion control.

for moving backward motion control, for observations on the system's displacement, velocity upon motions, torque on wheels and in between links, as well as angular positions of both Link1 and Link2. Primarily, a traveled distance of 12m has been seen following a velocity of 0.21m/s on the system's uphill stirring. While similar values on both dimensions are recorded in cases of disturbances from a single direction, positive forces, in this context, have demonstrated greater implications on the system's fluctuation, with proof of almost 0.4m/s in recorded velocity during the points of disturbance experienced (+500N at the 10s and 40s).

As shown in Fig. 16, the maximum overshoot and under-shoot for the magnitude of the torque on both wheels

and in between the system's links are acknowledged at $< \pm10\text{Nm}$ following disturbances from both directions, even though higher torque can be seen during the initial stage of the simulation. It is recorded that the torque starts to increase to +60Nm and −40Nm for both wheels and the system's links, but then it decreases dramatically. Higher initial torques are contributed by the controller managing the payload's momentum in kick-starting the inclined motions with the system maintaining a stable condition.

A similar situation happens to the angular positions of both links, whereby the magnitude of the angular position for the Link1 starts at −16°, which then decreases to approximately
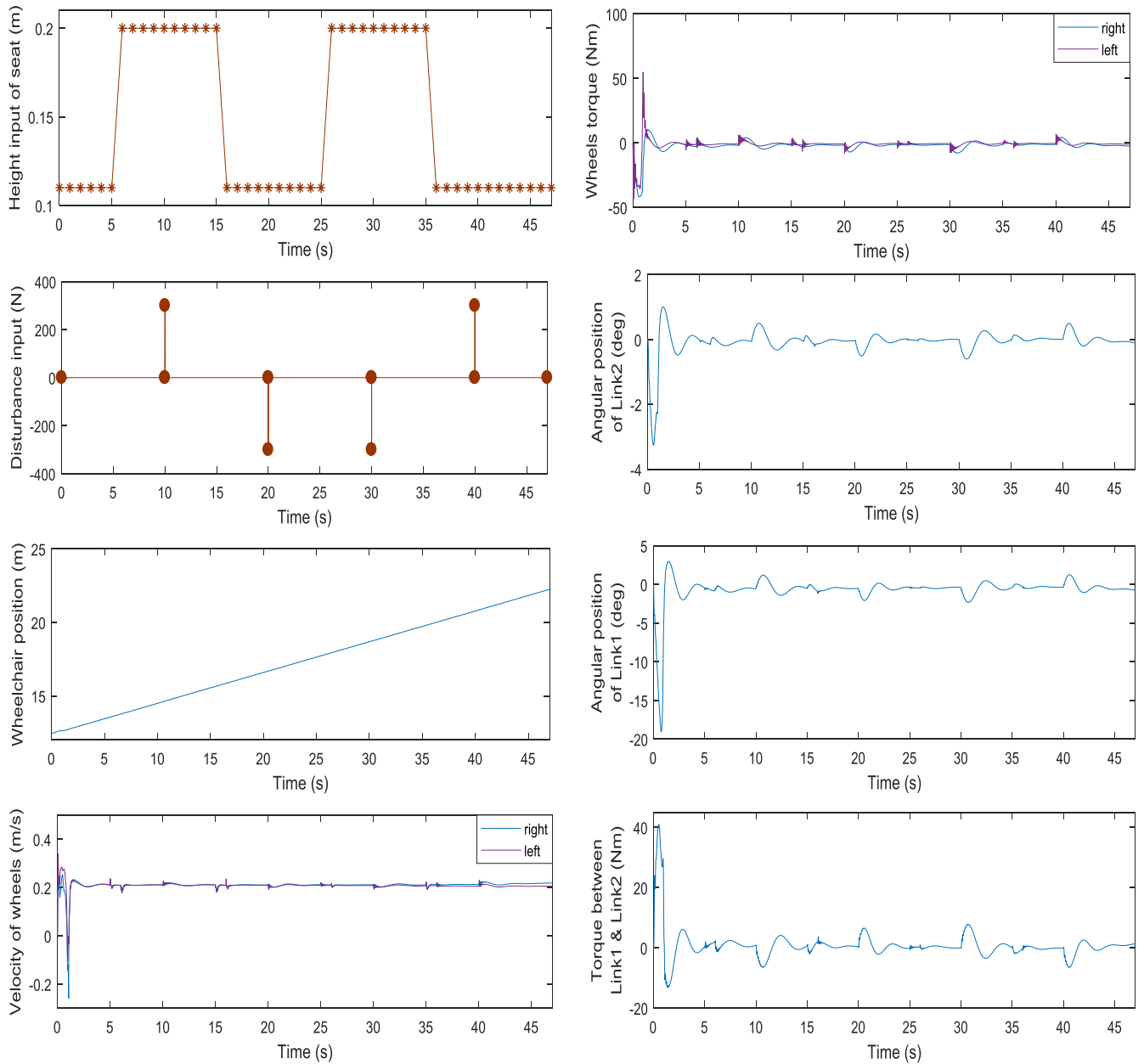
FIGURE 17. Performance of the system while moving downhill motion control.

±3° as the simulation proceeds. Meanwhile, the Link2 started at −3°, which then falls to < ±1°, respectively. The maximum overshoot and undershoot for both links are hit upon application of external disturbances at ±500N during specified points within the designated timeframe, with the system requiring <10s in settling time to regain its optimal 0°. With control being provided by the proposed SDA-IT2FLC approach, conditions had proven to be non-challenging, even when the disturbances involved simultaneously originate from diverging directions, with the concurrent involvement of a movable payload, and the system maneuvering in an uphill stir.

Ultimately, uncertainties in the uphill motions have been overcome by the proposed controller as implemented in the two-wheeled wheelchair system. More so, when the external disturbances and vertical changes in the payload's height are involved, SDA-IT2FLC has handled and rejected such uncertainties with considerable excellence, under the disturbance magnitude of up to 500N, originating either from single or multiple directions. With the inclined surface concerned, nonlinearity and complexity of the system, with environmental uncertainty, have proven the controller's ability to not only stabilize the two-wheeled on a uniform surface but also during an uphill climb.

F. PERFORMANCE OF SYSTEM FOR MOVING DOWNHILL MOTION CONTROL WITH POSITIVE AND NEGATIVE FORCES DISTURBANCE REJECTION

In completing the whole experiment in this paper, the robustness of SDA-IT2FLC, as implemented in a two-wheeled wheelchair system with movable payload is then tested with the application of both positive and negative disturbances to the back of the seat in a simulation for the moving downhill motion control, as shown in Fig. 17. However, unlike the moving uphill simulations, forces in a magnitude of ±300N were applied for the current experiment (5th experiment) instead. Even lower disturbances were applied for the 5th experiment, compared to the uphill inclined motions, to account for greater difficulties of the downhill motions undertaken by a system at the expense of the capability to handle higher external forces.

The height input to the system's payload is then presented in Fig. 17 with a maximum height of seat motions being 0.20m with a movable payload. Similarly, disturbances are applied as seen in 1) The 10s when the payload is extended to the maximum level of height near the peak of the slope, 2) the 20s when the payload is maintained without the extension (normal level) at a higher position of the slope, 3) the 30s when the payload extended to the maximum level of height at a position closer to the ground, and 4) the 40s when the payload is maintained without extension (normal level).

The system's performance for the moving downhill motion control has also been presented in Fig. 17, which outlined the system's displacement and velocity, torque on both wheels and between links, as well as the angular positions of the respective links. Similar to the forces being applied from a single direction, the system traveled a distance of up to 10m for the downhill maneuver, with the same velocity of 0.21m/s. Noted that forces are applied from diverging directions within the same simulation, smooth stirring can still be observed with heightened system stability.

In stabilizing the wheelchair's system for further downhill motions, higher values have also been recorded for maximum overshoot and undershoot at the initial phase of the simulation, with ±55Nm for the torque of both wheels, and ±41Nm for torque between Link1 and Link2. Priority is placed on the effort of SDA-IT2FLC to manage the payload's momentum and handle incoming uncertainties following the executed simulation. After being stabilized, the torque on both wheels and in between Link1 and Link2 fall to mere ±7Nm and ±8Nm.

The effectiveness of the proposed controller is further supported by the magnitude of the angular positions of both links, in which similar situations have occurred. The simulation starts with the angular positions of $-19°$ and $-3.3°$ for both the first and second links. These values are then reduced after the 3s, with an amplitude of respective links being recorded at only $\pm2°$ and $< \pm0.6°$ when faced with forces of ±300N. The fluctuations remain somewhat apparent; the disruptions settled within a 10s interval, which proves superiority in the performance of SDA-IT2FLC in rejecting

inconsistent disturbances, which further maintains stability, despite heightened nonlinearity and uncertainty of the operating system.

The proposed SDA-IT2FLC controller has demonstrated the uncanny capability of managing the upright stability of a two-wheeled wheelchair with a movable payload while making inclined motions downhill. Specifically, the system, through the implementation of the proposed controller, has successfully produced satisfactory results, in areas of stability, settling time, overshoot and undershoot, disturbance rejection, through applying the optimized control parameters. Given that the current experiments focused on understanding the effectiveness of the controller in rejecting external disturbances, forces from both singular and diverged directions are deemed manageable by SDA-IT2FLC during an inclined maneuver.

VI. CONCLUSION

In this paper, the enhanced IT2FLC approach used to stabilize a two-wheeled wheelchair with a movable payload in various conditions has been proposed, while the reconfiguration of the wheelchair modeled upon the SW4D environment. This proposed controller has been thoroughly implemented, and its robustness is intensively investigated in this paper. The system's performance is further observed in a comprehensively simulated exercise using the SW4D visualization software and Simulink in Matlab.

Through the experiments conducted, the system has been shown to withstand external disturbances at ±1000N in four different conditions; when the seat is at the maximum height of extension, when the seat is at its original state without extension, while the seat is moving up to reach its maximum height, and while the seat is moving down back to its original state. It has also been demonstrated that the performance of the system which adopts the optimized IT2FLC is better in terms of overshooting and undershooting when simulated with the optimized parameters through the use of SDA. This is shown through the recorded torques between Link1 and Link2 at a value of less than ±30Nm following external disturbances.

The proposed controller, which has optimized IT2FLC, produces low torques for both Link1 and Link2 after being perturbed by positive and negative disturbances between ±100N to ±300N and $+350$N. With the disturbance pattern that is similar to that of previous works simulated for the current study [6], [9], approximately 94% reduction in the torque between Link1 and Link2, and more than 98% reduction in the traveled distance have been acknowledged in comparison to the previous design (using FLCT1). This is due to the influence of external disturbance force. While previous studies emphasized the system with fixed payload (without carrying a payload in an upward and downward motion), the current paper has placed considerable thought into the case of a moving payload, which is far more complex in comparison. Even with the inclusion of external disturbances up to ±1000N, the maximum height transformations of the

height of the seat is at about 0.25m from 0.11m (normal level), a moving payload, as well as while the system is doing a forward motion and backward motion control, this study concludes that the SDA-IT2FLC controller has completely excelled in handling a system with heightened nonlinearities and uncertainties.

However, do note that while a moving system has been accounted for in this study, it is only limited to a flat and inclined surface. Therefore, the mechanism of a two-wheeled wheelchair that can be used to move upward and downward on other surfaces (sandy and gravel surfaces), with the applications of external disturbances and height transformation can be a distinct area for further exploration, while enhancing the safety and effectiveness of users in a real hardware application. Besides, the control mechanism during the modeling will look at further improvement as well as the simulation of the system.

REFERENCES

[1] S. Ahmad and M. O. Tokhi, "Linear Quadratic Regulator (LQR) approach for lifting and stabilizing of two-wheeled wheelchair," in *Proc. 4th Int. Conf. Mechatronics (ICOM)*, May 2011, pp. 1–6.

[2] N. M. A. Ghani, M. O. Tokhi, A. N. K. Nasir, and S. Ahmad, "Control of a stair climbing wheelchair," *Int. J. Robot. Automat.*, vol. 1, no. 4, pp. 203–213, 2012.

[3] S. Ahmad and M. O. Tokhi, "Modelling and control of a wheelchair on two wheels," in *Proc. 2nd Asia Int. Conf. Modelling Simulation (AMS)*, May 2008.

[4] S. Ahmad and M. O. Tokhi, "Forward and backward motion control of wheelchair on two wheels," in *Proc. 3rd IEEE Conf. Ind. Electron. Appl.*, Jun. 2008, pp. 461–466.

[5] M. El-Bardini and A. M. El-Nagar, "Interval type-2 fuzzy PID controller for uncertain nonlinear inverted pendulum system," *ISA Trans.*, vol. 53, no. 3, pp. 732–743 2014.

[6] S. Ahmad, N. H. Siddique, and M. O. Tokhi, "A modular fuzzy control approach for two-wheeled wheelchair," *J. Intell. Robot. Syst.*, vol. 64, nos. 3–4, pp. 401–426, 2011.

[7] S. Ahmad and M. O. Tokhi, "Steering motion control enhancement scheme of two wheeled wheelchair in confined spaces," *Int. J. Automat. Control Eng.*, vol. 2, no. 4, pp. 179–189 2013.

[8] N. M. A. Ghani and M. O. Tokhi, "Simulation and control of multipurpose wheelchair for disabled/elderly mobility," *Integr. Comput.-Aided Eng.*, vol. 23, no. 4, pp. 331–347 2016.

[9] S. Ahmad, N. H. Siddique, and M. O. Tokhi, "Modelling and simulation of double-link scenario in a two-wheeled wheelchair," *Integr. Comput.-Aided Eng.*, vol. 21, no. 2, pp. 119–132 2014.

[10] T. Altalmas, A. Aula, S. Ahmad, M. O. Tokhi, and R. Akmeliawati, "Integrated modeling and design for realizing a two-wheeled wheelchair for disabled," *Assistive Technol.*, vol. 28, no. 3, pp. 159–174, 2016.

[11] M. T. A. Rahman, S. Ahmad, R. Akmeliawati, T. Altalmas, and A. Aula, "Centre of gravity (COG)-based analysis on the dynamics of the extendable double-link two-wheeled mobile robot," in *Proc. 5th Int. Conf. Mechatronics*, 2013, pp. 1–9.

[12] A. M. Almeshal, K. M. Goher, and M. O. Tokhi, "Dynamic modelling and stabilization of a new configuration of two-wheeled machines," *Robot. Auton. Syst.*, vol. 61, Volume 61, no. 5, pp. 443–472, 2013.

[13] K. M. K. Goher and M. O. Tokhi, "Genetic algorithm based modeling and control of a two wheeled vehicle with an extended rod, a lagrangian based dynamic approach," in *Proc. IEEE 9th Int. Conf. Cyberntic Intell. Syst.*, Sep. 2010, pp. 1–6.

[14] M. T. A. Rahman, S. Ahmad, and R. Akmeliawati, "Integrated modeling and analysis of an extendable double-link two-wheeled mobile robot," in *Proc. IEEE/ASME Int. Conf. Adv. Intell. Mechatronics*, Jul. 2013, pp. 1798–1803.

[15] M. Nie and W. W. Tan, "Towards an efficient type-reduction method for interval type-2 fuzzy logic systems," in *Proc. IEEE Int. Conf. Fuzzy Syst. (IEEE World Congr. Comput. Intell.)*, 2008, pp. 1425–1432.

[16] D. Wu, "Approaches for reducing the computational cost of interval type-2 fuzzy logic systems: Overview and comparisons," *IEEE Trans. Fuzzy Syst.*, vol. 21, no. 1, pp. 80–99, 2013.

[17] N. M. A. Ghani, A. N. K. Nasir, and M. O. Tokhi, "Optimization of fuzzy logic scaling parameters with spiral dynamic algorithm in controlling a stair climbing wheelchair: Ascending task," in *Proc. 19th Int. Conf. Methods Models Automat. Robot. (MMAR)*, Sep. 2014, pp. 776–781.

[18] K. Tamura and K. Yasuda, "Primary study of spiral dynamics inspired optimization," *IEEJ Trans. Elect. Electron. Eng.*, vol. 6, no. 1, pp. 98–100, 2010.

[19] S. K. Yadav, S. Sharma, and N. Singh, "Optimal control of double inverted pendulum using LQR controller," *Int. J. Adv. Res. Comput. Sci. Softw. Eng.*, vol. 2, no. 2, pp. 189–192, 2012.

[20] N. Singh and S. K. Yadav, "Comparison of LQR and PD controller for stabilizing double inverted pendulum system," *Int. J. Eng. Res. Develop.*, vol. 1, no. 12, pp. 69–74 2012.

[21] T. Henmi, M. Deng, and A. Inoue, "Swing-up control of a serial double inverted pendulum," in *Proc. Amer. Control Conf.*, Jun./Jul. 2004, pp. 3992–3997.

[22] A. Bogdanov, "Optimal control of a double inverted pendulum on a cart," Dept. Comput. Sci. Elect. Eng., OGI School Sci. Eng., OHSU, Portland, OR, USA, Tech. Rep. CSE-04-006, 2004.

[23] H. Wei, Q. Qian, H. Qiang, H. Qiaoli, Z. Yixin, and X. Lin, "Optimization of sliding mode controller for double inverted pendulum based on genetic algorithm," in *Proc. 2nd Int. Symp. Syst. Control Aerosp. Astronaut.*, Dec. 2008, pp. 1–5.

[24] M. Lashin and A. Ramadan, "Optimal design of a state feedback sliding mode controller of a loaded double inverted pendulum," *IEEE Control Syst. Mag.*, early access, Oct. 6, 2015.

[25] M. Lashin, A. Ramadan, H. S. Abbass, and A. A. Ismail, "Design of an optimized sliding mode control for loaded double inverted pendulum with mismatched uncertainties," in *Proc. 19th Int. Conf. Methods Models Automat. Robot. (MMAR)*, Sep. 2014, pp. 270–275.

[26] M. Y. Hsiao and C. T. Wang, "A finite-time convergent interval type-2 fuzzy sliding-mode controller design for omnidirectional mobile robots," in *Proc. Int. Conf. Adv. Robot. Intell. Syst.*, May/Jun. 2013, pp. 80–85.

[27] H. A. Hagras, "A hierarchical type-2 fuzzy logic control architecture for autonomous mobile robots," *IEEE Trans. Fuzzy Syst.*, vol. 12, no. 4, pp. 524–539, Aug. 2004.

[28] U. Farooq, J. Gu, and J. Luo, "An interval type-2 fuzzy LQR positioning controller for wheeled mobile robot," in *Proc. IEEE Int. Conf. Robot. Biomimetics (ROBIO)*, Dec. 2013, pp. 2403–2407.

[29] M. H. Ri and J. Huang, "Design of interval type-2 fuzzy logic controller for mobile wheeled inverted pendulum," in *Proc. 12th World Congr. Intell. Control Automat. (WCICA)*, Jun. 2016, pp. 535–540.

[30] A. M. El-Nagar, M. El-Bardini, and N. M. El-Rabaie, "Intelligent control for nonlinear inverted pendulum based on interval type-2 fuzzy PD controller," *Alexandria Eng. J.*, vol. 53, no. 1, pp. 23–32 2014.

[31] M. Y. Hsiao, C. Y. Chen, and T. H. S. Li, "Interval type-2 adaptive fuzzy sliding-mode dynamic control design for wheeled mobile robots," *Int. J. Fuzzy Syst.*, vol. 10, no. 4, pp. 268–275 2008.

[32] J. M. Mendel and F. Liu, "Super-exponential convergence of the Karnik–Mendel algorithms for computing the centroid of an interval type-2 fuzzy set," *IEEE Trans. Fuzzy Syst.*, vol. 15, no. 2, pp. 309–320, Apr. 2007.

[33] D. Wu and J. M. Mendel, "Enhanced Karnik–Mendel algorithms," *IEEE Trans. Fuzzy Syst.*, vol. 17, no. 4, pp. 923–934, Aug. 2009.

[34] H. Wu and J. M. Mendel, "Uncertainty bounds and their use in the design of interval type-2 fuzzy logic systems," *IEEE Trans. Fuzzy Syst.*, vol. 10, no. 5, pp. 622–639, Oct. 2002.

[35] M. B. Begian, W. W. Melek, and J. M. Mendel, "Stability analysis of type-2 fuzzy systems," in *Proc. IEEE Int. Conf. Fuzzy Syst. (IEEE World Congr. Comput. Intell.)*, Jun. 2008, pp. 947–953.

[36] K. Duran, H. Bernal, and M. Melgarejo, "Improved iterative algorithm for computing the generalized centroid of an interval type-2 fuzzy set," in *Proc. Annu. Meeting North Amer. Fuzzy Inf. Process. Soc.*, May 2008, pp. 1–5.

[37] M. Melgarejo, "A fast recursive method to compute the generalized centroid of an interval type-2 fuzzy set," in *Proc. Annu. Meeting North Amer. Fuzzy Inf. Process. Soc.*, Jun. 2007, pp. 190–194.

[38] D. Wu and M. Nie, "Comparison and practical implementation of type-reduction algorithms for type-2 fuzzy sets and systems," in *Proc. IEEE Int. Conf. Fuzzy Syst.*, 2011, pp. 2131–2138.

[39] K. A. Naik and C. P. Gupta, "Performance comparison of Type-1 and Type-2 fuzzy logic systems," in *Proc. 4th Int. Conf. Signal Process., Comput. Control (ISPCC)*, Sep. 2017, pp. 72–76.

[40] O. Castillo, L. Amador-Angulo, R. C. R. C. Juan Mario GV Juan, and G. V. Mario, "A comparative study of type-1 fuzzy logic systems, interval type-2 fuzzy logic systems and generalized type-2 fuzzy logic systems in control problems," *Inf. Sci.*, vol. 354, pp. 257–274, Aug. 2016.

[41] P. E. Hsu, Y. L. Hsu, J. M. Lu, and C.-H. Chang, "Seat adjustment design of an intelligent robotic wheelchair based on the stewart platform," *Int. J. Adv. Robot. Syst.*, vol. 10, no. 3, p. 168, Mar. 2013, doi: 10.5772/55880.

[42] D. Piovesan, M. Yagiela, R. Johnson, and A. Schmitz, "Combining Gait Trainers and Partial Weight Bearing Lifters: A Dynamic Analysis of Seat-to-Stand Transition," in *Proc. ASME Dyn. Syst. Control Conf.*, 2017, Art. no. V001T07A001, doi: 10.1115/dscc2016-9731.

[43] H.-C. Yang, "Using an imaginary planar rack cutter to create a spherical gear pair with continue involute teeth," *Arabian J. Sci. Eng.*, vol. 42, no. 11, pp. 4725–4735, Nov. 2017, doi: 10.1007/s13369-017-2630-z.

[44] K. Tamura and K. Yasuda, "Spiral optimization -A new multipoint search method," in *Proc. IEEE Int. Conf. Syst., Man, Cybern.*, vol. 1, Oct. 2011, pp. 1759–1764.

[45] X. H. Chang, Y. Can, and J. Xiong, "Quantized fuzzy output feedback H∞ control for nonlinear systems with adjustment of dynamic parameters," *IEEE Trans. Syst., Man, Cybern., Syst.*, vol. 49, no. 10, pp. 2005–2015, Oct. 2019.

[46] M. Dirik, O. Castillo, and A. F. Kocamaz, "Visual-servoing based global path planning using interval type-2 fuzzy logic control," *Axioms*, vol. 8, no. 2, p. 58, 2019.

[47] E. Ontiveros-Robles, P. Melin, and O. Castillo, "Comparative analysis of noise robustness of type 2 fuzzy logic controllers," *Kybernetika*, vol. 54, no. 1, pp. 175–201, Mar. 2018.

NOR MANIHA ABDUL GHANI received the B.Eng. and M.Eng. degrees from Universiti Teknologi Malaysia, in 2003 and 2006, respectively, and the Ph.D. degree from The University of Sheffield, U.K., in 2015. She is currently a Senior Lecturer and also serving an Electrical and Electronics Programme with the Faculty of Electrical & Electronics Engineering, Universiti Malaysia Pahang. Her current research interests include model and system control, control parameter optimization, balancing stability control, and intelligent and fuzzy logic control.

NURUL FADZLINA JAMIN received the B.Eng. degree from Universiti Malaysia Pahang, in 2012, and the M.Eng. degree from Universiti Tun Hussein Onn Malaysia, in 2014. She is currently pursuing the Ph.D. degree with the Faculty of Electrical & Electronics Engineering, Universiti Malaysia Pahang. Her research interests include fuzzy system, balancing stability control, and optimization of control parameter.

ZUWAIRIE IBRAHIM received the B.Eng. and M.Eng. degrees from Universiti Teknologi Malaysia, in 2000 and 2002, respectively, and the Ph.D. degree from Meiji University, Japan, in 2006. He is currently an Associate Professor and also serving a Mechatronics Programme with the Engineering College, Universiti Malaysia Pahang. His current research interests include computational intelligence, artificial intelligence, and data estimation.

• • •